Available online at www.sciencedirect.com
SCIENCE DIRECT
Journal of Organometallic Chemistry 691 (2006) 2614–2622
Journal of Organometallic Chemistry
www.elsevier.com/locate/jorganchem

Molecular architectures of cationic $[Pd(\eta^3\text{-}C_3H_5)(pz^{bp2}py)]^+$ complexes and BF_4^- and $CF_3SO_3^-$ as counteranions ($pz^{bp2}py$ = 2-[3,5-bis(4-butoxyphenyl)pyrazol-1-yl]pyridine)

M.C. Torralba [a], M. Cano [a,*], J.A. Campo [a], J.V. Heras [a], E. Pinilla [a,b], M.R. Torres [b], J. Perles [c], C. Ruiz-Valero [c]

[a] Departamento de Química Inorgánica I, Facultad de Ciencias Químicas, Universidad Complutense, E-28040 Madrid, Spain
[b] Laboratorio de Difracción de Rayos-X, Facultad de Ciencias Químicas, Universidad Complutense, E-28040 Madrid, Spain
[c] Instituto de Ciencia de Materiales, CSIC, Cantoblanco, E-28049 Madrid, Spain

Received 12 November 2005; received in revised form 20 December 2005; accepted 20 December 2005
Available online 10 March 2006

Abstract

The crystal structures of two complexes containing the 2-[3,5-bis(4-butoxyphenyl)pyrazol-1-yl]pyridine ($pz^{bp2}py$) ligand bonded to the $[Pd(\eta^3\text{-}C_3H_5)]^+$ fragment and BF_4^- and $CF_3SO_3^-$ as counteranions (**1** and **2**, respectively) have been solved and their molecular architectures compared. The compounds exhibit a ^{2}D network based on weak interactions in which the counterion plays an important role. The molecular layers in the ^{2}D arrangement show interpenetration between the substituent-chains on the pyrazole rings. These features are also observed in related compounds bearing only one chain on the pyrazole ring.

Keywords: Palladium(II) complexes; Pyrazolylpyridine ligands; X-ray structure; Supramolecular architecture

1. Introduction

A variety of multidimensional frameworks have been constructed by coordination bonds between multifunctional ligands and metal ions in different coordination environments. Other synthetic approaches such as those based on hydrogen bonds or $\pi\cdots\pi$ interactions have also been used and are well documented [1,2]. In general, supramolecular architectures assembled by coordination bonds or supramolecular interactions have been proposed to be useful for more predictable control over directional assemblies and packing in the solid state [1].

In addition, weaker interactions have also been exploited in crystal engineering studies [3], and due to their abundance in the crystal structures, their contribution should also be considered in the design of supramolecular architectures.

In previous works from our lab, we have found that the crystallization process of complexes of the type $[Pd(\eta^3\text{-}C_3H_5)(Hpz^*)_2]A$ containing the $[Pd(\eta^3\text{-}C_3H_5)]^+$ fragment and pyrazole groups (Hpz^* = 3,5-bis(4-butoxyphenyl)pyrazole Hpz^{bp2}; 3,5-dimethyl-4-nitropyrazole Hpz^{NO2}) as co-ligands was strongly controlled by hydrogen bonding interactions established between the counterions, A, and the NH pyrazolic groups [4,5]. By contrast, in the related compounds $[Pd(\eta^3\text{-}C_3H_5)(pz^Rpy)]A$ (pz^Rpy = 2-[3-(4-alkyloxyphenyl)pyrazol-1-yl]pyridine; A = BF_4^-, PF_6^-, $CF_3SO_3^-$), the pz^Rpy ligands can only act as terminal ligands as they form bidentate chelating species [6]. In the absence of

* Corresponding author. Fax: +34 91 3944352.
E-mail address: mmcano@quim.ucm.es (M. Cano).

0022-328X/$ - see front matter © 2006 Elsevier B.V. All rights reserved.
doi:10.1016/j.jorganchem.2005.12.071

NH groups, these ligands do not have supramolecular interaction sites for molecular recognition through NH···A bonds. In spite of these, the counterion still plays an important role at a supramolecular level involving non-conventional C–H···F hydrogen bonds between neighbouring entities which produce polymeric chains in a ^{1}D assembly (Fig. 1). Additional related interactions hold the chains together defining molecular layers. These features, which were observed in the crystal structures of $[Pd(\eta^3\text{-}C_3H_5)(pz^Rpy)]BF_4$ (pz^Rpy = 2-[3-(4-hexyloxyphenyl)pyrazol-1-yl]pyridine $pz^{hp}py$; 2-[3-(4-decyloxyphenyl)pyrazol-1-yl]pyridine $pz^{dp}py$), allowed us to establish that the bidentate pz^Rpy ligands and the counterion function as hydrogen-bond sources giving rise to a ^{2}D supramolecular assembly [6].

Since layer-like molecular assemblies in the solid state can be related to the lamellar structures of liquid crystal compounds, the above structural features are potentially useful to establish structure/mesomorphic properties relationships in metallomesogenic coordination compounds based on mesogenic or promesogenic pyrazolylpyridine-type ligands [7].

Following these results, we are now interested in proving that a similar structural behavior can be obtained in related complexes with adequate counterions, thus contributing to the design of layer-like structures based on weak non-conventional hydrogen-bonds. Taking into account the supramolecular structure of $[Pd(\eta^3\text{-}C_3H_5)(pz^{hp}py)]BF_4$ [6], we expect that the presence of two substituents at the 3 and 5 positions of the pyrazole group should not significantly modify the molecular assembly through the counterion, at least in the ^{1}D arrangement (Fig. 1).

In this work, the X-ray structures of the complexes $[Pd(\eta^3\text{-}C_3H_5)(pz^{bp2}py)]A$ (A = BF_4^- **1**, $CF_3SO_3^-$ **2**) containing disubstituted pyrazole groups ($pz^{bp2}py$ = 2-[3,5-bis(4-butoxyphenyl)pyrazol-1-yl]pyridine) have been solved and the molecular assemblies discussed. We were also interested in establishing how counterions such as BF_4^- or $CF_3SO_3^-$ could contribute to the formation of ^{1}D assemblies through hydrogen-bond interactions involving the F and/or O atoms. Further interactions were expected to extend the dimensionality to a ^{2}D framework.

2. Experimental

2.1. Materials and physical measurements

All commercial reagents were used as supplied. The starting Pd-complex $[Pd(\mu\text{-}Cl)(\eta^3\text{-}C_3H_5)]_2$ was purchased from Sigma–Aldrich and used as supplied. The ligand 2-[3,5-bis(4-butoxyphenyl)pyrazol-1-yl]pyridine ($pz^{bp2}py$) and compound **1** were prepared as described in the literature [4,8].

Elemental analyses for carbon, hydrogen, nitrogen and sulphur were carried out by the Microanalytical Service of the Complutense University. IR spectra were recorded on a FTIR ThermoNicolet 200 spectrophotometer with samples as KBr pellets in the 4000–400 cm^{-1} region.

^{1}H NMR spectra were performed on a Bruker AC-200 spectrophotometer (NMR Service of the Complutense

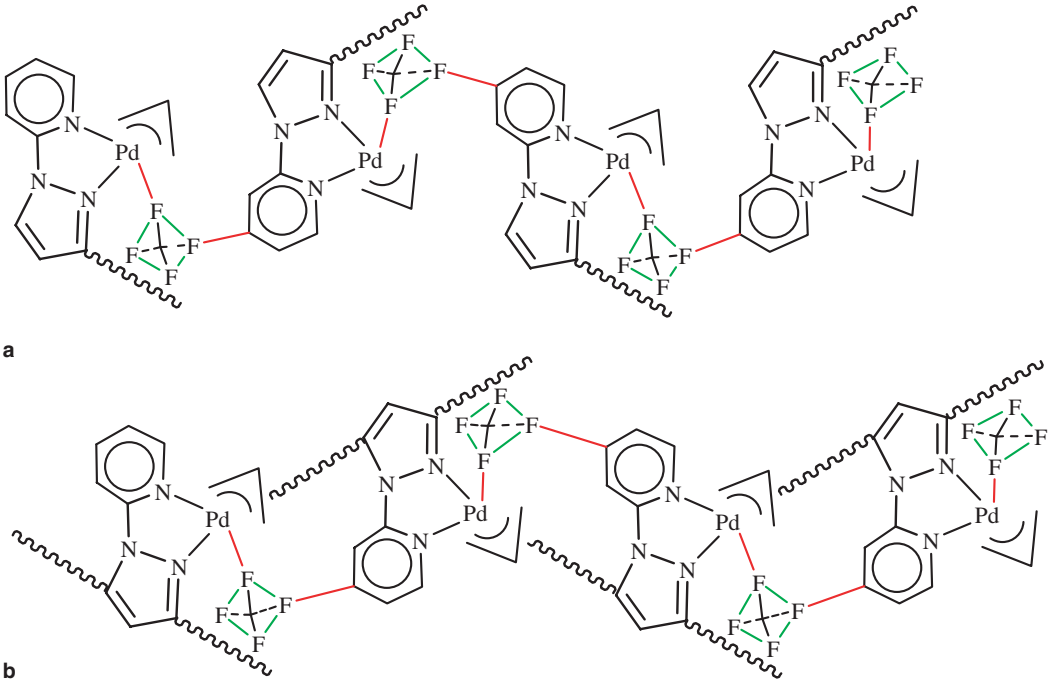

Fig. 1. (a) Schematic representation of the structure of $[Pd(\eta^3\text{-}C_3H_5)(pz^Rpy)]BF_4$ (pz^Rpy = 2-[3-(4-alkyloxyphenyl)pyrazol-1-yl]pyridine) [6]. (b) Schematic representation of the proposed structure for $[Pd(\eta^3\text{-}C_3H_5)(pz^{R2}py)]BF_4$ ($pz^{R2}py$ = 2-[3,5-bis(4-alkyloxyphenyl)pyrazol-1-yl]pyridine).

University) from solutions in $CDCl_3$. Chemical shifts δ are listed in ppm relative to TMS using the signal of the deuterated solvent as reference (7.26 ppm), and coupling constants J are in hertz. Multiplicities are indicated as d (doublet), t (triplet), m (multiplet), br (broad signal). The ^1H chemical shifts and coupling constants are accurate to ±0.01 ppm and ±0.3 Hz, respectively.

2.2. Preparation of $[Pd(\eta^3\text{-}C_3H_5)(pz^{bp2}py)]CF_3SO_3$

To a solution of $[Pd(\mu\text{-}Cl)(\eta^3\text{-}C_3H_5)]_2$ (0.107 mmol, 39 mg) in 20 mL of acetone, $AgSO_3CF_3$ (0.214 mmol, 54.8 mg) was added. The mixture of reaction was stirred at room temperature under nitrogen and absence of light at least for six hours. Then the residue was separated by filtration over celite and $pz^{bp2}py$ (0.214 mmol, 94.1 mg) dissolved in ca. 10 ml of dichloromethane was added to the resulting colorless solution. After 24 h stirring at room temperature under nitrogen, the solution was filtered over celite/activated carbon and the solvent partially removed in vacuo. The addition of hexane led to the crystallization of colorless needles that were isolated by filtration, washed with hexane and dried in vacuo. Yield: 60%.

Elemental analyses: found C 52.0, H 5.0, N 5.8, S 4.3%; calculated for $C_{32}H_{36}F_3N_3O_5SPd$: C 52.1, H 4.9, N 5.7, S 4.3%. IR (KBr, cm^{-1}): ν(CN) 1610, $\gamma(CH)_{py}$ 770, $\nu(SO_3) + \nu(CF_3)$ 1272–1253, $\nu_s(SO_3)$ 1027. ^1H NMR ($CDCl_3$; δ in ppm; J, in Hz): 8.89 (dd, $^3J = 5.4$, $^4J = 1.0$, 1H, H6(py)), 7.81 (ddd, $^3J = 8.5$, $^3J = 6.8$, $^4J = 1.7$, 1H, H4(py)), 7.59 (d, $^3J = 8.8$, 2H, H*o*(C_6H_4)), 7.54 (ddd, $^3J = 6.6$, $^3J = 5.4$, $^4J = 1.0$, 1H, H5(py)), 7.41 (d, $^3J = 8.8$, 2H, H*o*(C_6H_4)), 7.06 (d, $^3J = 8.8$, 2H, H*m*(C_6H_4)), 7.04 (d, $^3J = 8.8$, 2H, H*m*(C_6H_4)), 6.99 (d, $^3J = 8.6$, 1H, H3(py)), 6.69 (s, 1H, H4(pz)), 5.70 (m, $^3J_a = 12.7$, $^3J_s = 6.8$, 1H, H*meso*(C_3H_5)), 4.06 (t, $^3J = 6.4$, 2H, OCH_2), 4.05 (t, $^3J = 6.3$, 2H, OCH_2), 4.05 (2H, H*s*(C_3H_5), masked by the OCH_2 signals), 3.35 (br, 2H, H*a*(C_3H_5)), 1.83 (m, 4H, CH_2), 1.54 (m, 4H, CH_2), 1.01 (t, $^3J = 7.2$, 6H, CH_3).

2.3. X-ray structure determinations of $[Pd(\eta^3\text{-}C_3H_5)(pz^{bp2}py)]A$ ($A = BF_4^-$ **1**, $CF_3SO_3^-$ **2**)

Suitable pale yellow or colorless crystals of **1** and **2**, respectively, were grown by layering dichloromethane solutions with hexane. The crystals were mounted on a Smart CCD-Bruker diffractometer with graphite monochromated Mo Kα radiation (λ 0.71073 Å) operating at 50 kV and 20 mA. A summary of the fundamental crystal and refinement data for these structures is given in Table 1.

In both cases, data were collected over an hemisphere of the reciprocal space by combination of the three exposure sets. Each exposure of 20 s covered 0.3° in ω. The cell parameters were determined and refined by a least-squares fit of all reflections. The first 100 frames were recollected at the end of the data collection to monitor crystal decay, and no appreciable decay was observed.

Table 1
Crystal and refinement data for **1** and **2**.

	1	**2**
Empirical formula	$C_{31}H_{36}BF_4N_3O_2Pd$	$C_{32}H_{36}F_3N_3O_5SPd$
Formula weight	675.84	738.13
Crystal system	Orthorhombic	Triclinic
Space group	*P*bca	$P(-1)$
a (Å)	9.961(1)	10.774(1)
b (Å)	19.824(2)	17.482(1)
c (Å)	31.062(3)	18.548(1)
α (°)		105.861(1)
β (°)		90.560(2)
γ (°)		101.547(2)
V (Å^3)	6134(1)	3284.9(4)
Z	8	4
T (K)	173(2)	296(2)
$F(000)$	2768	1512
$\rho_{calc.}$ (g cm^{-3})	1.464	1.492
μ (mm^{-1})	0.662	0.689
Crystal dimensions (mm)	$0.50 \times 0.40 \times 0.30$	$0.25 \times 0.12 \times 0.04$
Scan technique	ω and ϕ	ω and ϕ
Data collected	$(-14, -24, -30)$ to $(14, 28, 44)$	$(-12, -18, -21)$ to $(12, 20, 22)$
θ range (°)	3.76–31.09	1.14–25.00
Reflections collected	37883	25551
Independent reflections (R_{int})	9076 (0.0644)	11256 (0.0998)
Completeness to maximum θ (%)	92.0	97.4
Data/restraints/parameters	9076/0/497	11256/0/765
Observed reflections [$I \geqslant 2\,\sigma(I)$]	5895	4139
GOF (F^2)	1.077	0.809
R^a	0.0535	0.0575
$Rw_F{}^b$	0.1202	0.1272
Largest residual peak (e Å^{-3})	0.647	0.915

[a] $\sum[|F_o| - |F_c|]/\sum|F_o|$.

[b] $\{\sum[w(F_o^2 - F_c^2)^2]/\sum[w(F_o^2)^2]\}^{1/2}$.

Data for compound **1** were taken at low temperature (173 K). The structure was solved by direct methods and refined in the orthorhombic system (space group *P*bca). The refinement was made by full-matrix least-squares with anisotropical thermal parameters for all non-hydrogen atoms. In one of the butoxy chains, the three final atoms (C29, C30 and C31) show disorder, occupying two alternative positions A and B with a probability value of 51% and 49%, respectively. The hydrogen atoms of this fragment as well as the three hydrogen atoms bonded to C21 have been calculated and refined as riding on their respective carbon atoms. The remaining hydrogen atoms were located in a difference Fourier synthesis, included and refined their coordinates.

The structure of **2** was solved by direct and difference Fourier methods. Due to the existence of two crystallographic independent set of atoms which are apparently equal, data collection of different crystals and refinement with the original unit cell and a transform unit cell ($a = 10.680(1)$, $b = 10.771(1)$, $c = 17.127(1)$ Å; $\alpha = 80.158(2)$, $\beta = 73.844(1)$, $\gamma = 60.299(1)$°; $V = 1642.5(3)$ Å^3) were carried out. The same structural model was obtained in the acentric space group ($P1$) with the trans-

form unit cell, but the thermal parameters of many atoms became negative in the refinement. Thus, the refinement was made with the original cell by full-matrix least squares on F^2. All non-hydrogen atoms have been refined anisotropically, except some carbon atoms of the butoxy chains and the fluorine atoms of the $CF_3SO_3^-$ group. Hydrogen atoms were included in calculated positions and were refined as riding on their respective carbon atoms.

All calculations were performed using SMART software for data collection, SAINT for data reduction [9], and SHELXTL to resolve and refine the structure [10].

The refinement converged to R values of 0.0535 and 0.0575 for **1** and **2**, respectively. The largest residual peaks in the final difference map were 0.647 e $Å^{-3}$ for **1**, in the vicinity of the C9 atom, and 0.915 e $Å^{-3}$ for **2**, in the vicinity of the F1A atom.

3. Results and discussion

The synthesis and characterization of compound **1** have already been published by us [4]. Following a similar procedure, compound **2** was prepared from $[Pd(\eta^3\text{-}C_3H_5)(acetone)_2]CF_3SO_3$, which was obtained in situ by reaction of the dimer $[Pd(\mu\text{-}Cl)(\eta^3\text{-}C_3H_5)]_2$ and $AgCF_3SO_3$ in acetone [11]. Elemental analysis and IR and ^1H spectroscopic data agree with the proposed formulation (see Section 2).

Crystals of **1** and **2** suitable for X-ray diffraction were obtained from dichloromethane/hexane solutions. The structures of both compounds were unequivocally determined by single crystal X-ray diffraction.

Compound **2** presents two crystallographically independent sets of atoms in the asymmetric unit (namely **2A** and **2B**), which show significant differences in the relative disposition of the butoxy chains. Thus, the angle between the chains defined by the lines linking the corresponding CH_3 carbon atom and the oxygen atom is 73.6(3)° and 42.7(3)° for **2A** and **2B**, respectively.

The molecular structures of **1** and **2** consist of discrete $[Pd(\eta^3\text{-}C_3H_5)(pz^{bp2}py)]^+$ cations and BF_4^- or $CF_3SO_3^-$ anions, respectively (Figs. 2 and 3). In both cases, the cationic entity shows the same structural skeleton. Table 2 lists selected bond distances and angles, and Table 3 recovers the geometrical parameters for the C–H···F/O interactions responsible for the supramolecular arrangement.

The cations in **1** and **2** (**2A** and **2B**) each exhibits a pyrazolylpyridine ligand bonded in a bidentate manner through the N1 (N-pyrazole) and N3 (N-pyridine) atoms to the metal center giving rise to a five-membered metallocycle. The allyl ligand (π-bonded to the metal center) completes the coordination environment of the metal, which is distorted square-planar, with the Pd atom deviating −0.088(2) Å from the least-squares plane defined by the N1, N3, C1 and C3 atoms in the case of **1**, and 0.087(1) and −0.090(1) Å in **2A** and **2B**, respectively. The Pd1N1N3 and Pd1C1C3 planes are almost parallel (the dihedral angles are of 8.0(2)°, 7.2(2)° and 6.4(2)° for **1**, **2A** and **2B**, respectively).

The Pd–N distances (Table 2) are similar to those found in related compounds [4–6,11–13]. The Pd–N1 and Pd–N3 bonds form the basis of the five-membered chelate ring, with the Pd–N3 distance (mean value of 2.089 Å) being slightly shorter than the Pd–N1 one (mean value of 2.109 Å), in agreement with the expected difference in basicity of their respective heterocycles.

The C1C2C3 allyl group is slightly deviated from the ideal geometry (i.e., the mean values of the C–C bond distances and C–C–C angles are of ca. 1.39 Å and 118°, respectively; Table 2). The Pd–C(allyl) distances (2.092–2.126 Å) are in the expected range for a $[Pd(\eta^3\text{-allyl})]^+$ fragment with nitrogen ligands in *trans* position [5,6,11,12].

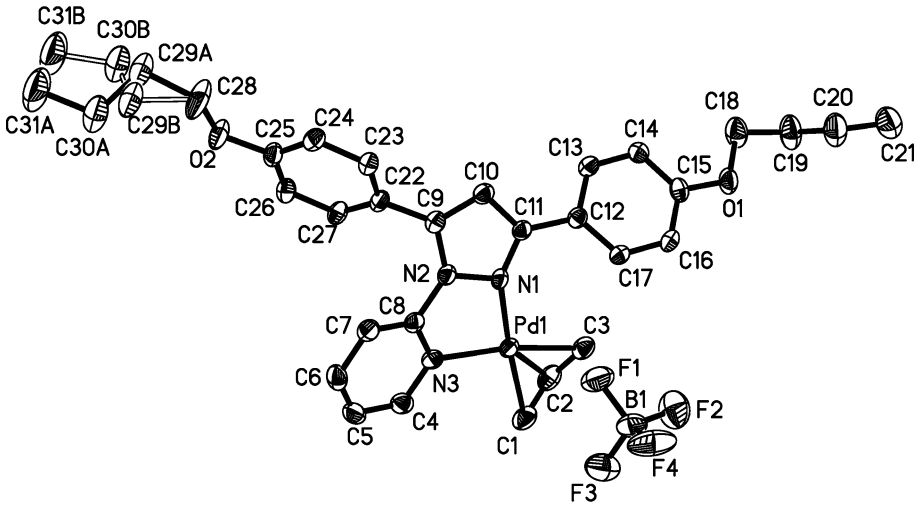

Fig. 2. ORTEP plot of **1** with 50% probability, showing the two alternative positions of C29, C30 and C31 atoms. Hydrogen atoms have been omitted for clarity.

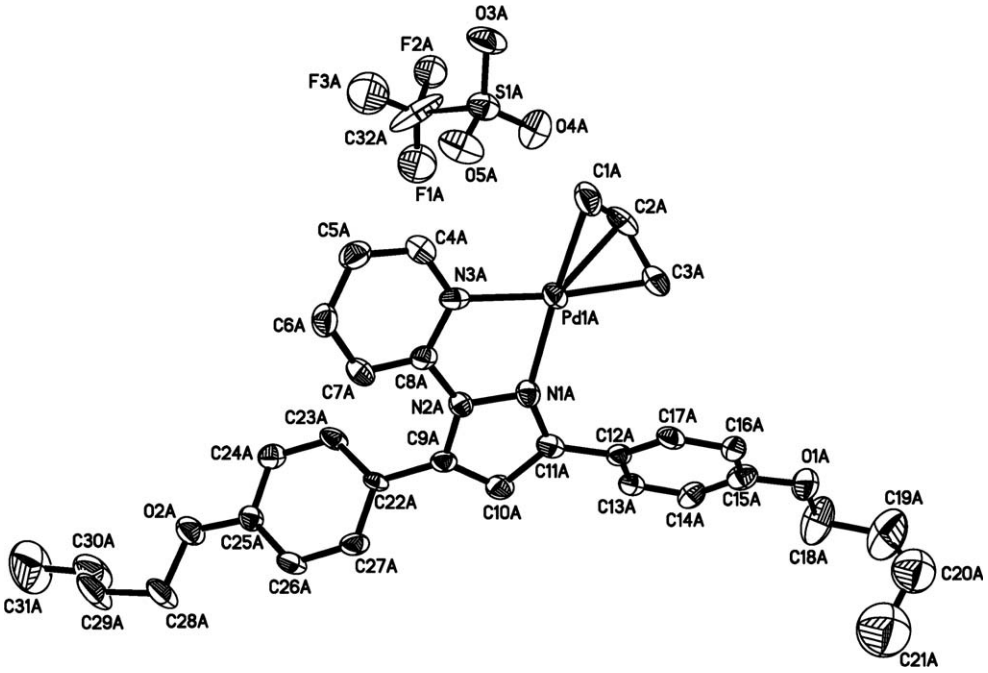

Fig. 3. ORTEP plot of **2A** with 40% probability. Hydrogen atoms have been omitted for clarity. The ORTEP plot of **2B** is similar and then it is not depicted.

Table 2
Selected bond distances (Å) and angles (°) for [Pd(η^3-C_3H_5)(pz^{bp2}py)]A (A = BF_4^- **1**; $CF_3SO_3^-$ **2**)

	1	2A	2B
Pd1–N1	2.118(2)	2.101(7)	2.107(6)
Pd1–N3	2.101(2)	2.093(7)	2.074(6)
Pd1–C1	2.123(3)	2.111(8)	2.113(8)
Pd1–C2	2.118(3)	2.113(8)	2.109(8)
Pd1–C3	2.122(3)	2.126(8)	2.092(8)
C1–C2	1.379(5)	1.39(1)	1.39(1)
C2–C3	1.393(5)	1.39(1)	1.37(1)
N1–Pd1–N3	77.89(9)	77.0(3)	77.5(3)
N1–Pd1–C1	171.9(1)	172.9(3)	173.8(3)
N1–Pd1–C2	144.2(1)	143.8(4)	143.3(4)
N1–Pd1–C3	110.4(1)	110.3(3)	110.5(3)
N3–Pd1–C1	103.6(1)	103.9(3)	103.2(3)
N3–Pd1–C2	134.6(1)	135.8(4)	136.1(4)
N3–Pd1–C3	171.5(1)	172.2(3)	170.9(3)
C1–Pd1–C2	37.9(1)	38.5(3)	38.5(3)
C1–Pd1–C3	67.9(1)	68.6(3)	68.4(3)
C2–Pd1–C3	38.4(1)	38.3(3)	38.0(3)
C1–C2–C3	117.6(4)	118.0(9)	118(1)

Table 3
Geometrical parameters for the weak C–H···F/O hydrogen-bond interactions (lengths in Å and angles in degrees) for [Pd(η^3-C_3H_5)(pz^{bp2}py)]A (A = BF_4^- **1**; $CF_3SO_3^-$ **2**)

Contact	*d*(D–H)	*d*(H···A)	*d*(D···A)	∠(D–H···A)
1				
C13–H···F4[a]	0.93(3)	2.54(3)	3.061(4)	116(2)
C4–H···F4[b]	0.95(3)	2.72(3)	3.149(4)	108(2)
C6–H···F2[c]	0.84(3)	2.59(3)	3.185(4)	129(3)
2				
C17A–H···O4B[d]	0.93	2.70	3.22(1)	120.8
C17B–H···O3A[e]	0.93	2.55	3.27(1)	134.4
C13A–H···O5A[f]	0.93	2.72	3.32(1)	123.1
C6A–H···F2A[g]	0.93	2.67	3.28(1)	123.1

[a] $1 + 1/2 - x, y + 1/2, z + 1$.
[b] $x - 1/2, 1 + 1/2 - y, 1 - z$.
[c] $x + 1/2, 1 + 1/2 - y, 1 - z$.
[d] $x, y + 1, z$.
[e] $x, y - 1, z$.
[f] $1 - x, 2 - y, -z$.
[g] $x + 1, y, z$.

The dihedral angle between the allyl plane (C1C2C3) and the coordination plane defined by the Pd, N1 and N3 atoms is 63.9(3)° for **1**, and 63.3(7) and 62.2(7)° for **2A** and **2B**, respectively, with the allyl carbon atoms displaced a mean value of 0.27 Å with respect to the PdN1N3 plane.

The pyrazole and pyridine planes are twisted respect to each other and form dihedral angles of 22.5(2)°, 19.0(2)° and 19.7(2)° for **1**, **2A** and **2B**, respectively. The benzene planes of the substituents are also twisted with respect to their own pyrazole planes with dihedral angles of 32.1(1)° and 48.3(1)° for **1**, 35.5(3)° and 51.7(2)° for **2A**, and 35.6(2)° and 55.0(2)° for **2B**. The largest angle in each compound corresponds, as expected, to the benzene plane closer to the pyridine ring. In this disposition, the benzene planes are twisted respect to each other at an angle of 74.2(1)°, 80.5(2)° and 85.5(2)° for **1**, **2A** and **2B**, respectively.

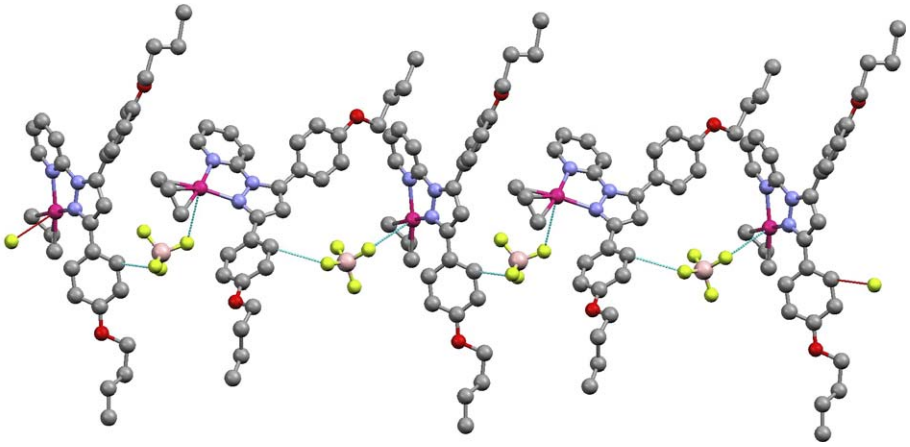

Fig. 4. View of the chain of **1** along the *b* axis, showing the Pd···F and C···F contacts.

At the supramolecular level, each BF_4^- anion in **1** is attached to two neighbouring cations through weak coordinative Pd···F1($x, y+1, z+1$) and non-conventional C13···F4($1+1/2-x, y+1/2, z+1$) hydrogen-bond interactions of 3.311(2) and 3.061(4) Å, respectively (Table 3). These interactions are propagated along the *b* axis, thus generating a polymeric chain with Pd···Pd distances of ca. 10.9 Å, in which the molecules involved show an inverse orientation (Fig. 4).

Further weak C···F hydrogen-bond interactions from different chains, involving the F2 and F4 atoms of the BF_4^- anion and the C4 and C6 atoms of the pyridine ring [C4···F4($x-1/2, 1+1/2-y, 1-z$) 3.149(4) Å, C6···F2-($x+1/2, 1+1/2-y, 1-z$) 3.185(4) Å] are also observed (Table 3). The chains are held together in layers, which are almost parallel to the *ab* plane (Fig. 5). In this layer-like structure the flexible chains are interdigitated, occupying the space between the layers (Fig. 6).

All the above structural features are similar to those found in the related complex $[Pd(\eta^3\text{-}C_3H_5)(pz^{hp}py)]BF_4$, with a monosubstituted pyrazole group ($pz^{hp}py$ = 2-[3-(4-hexyloxyphenyl)pyrazol-1-yl]pyridine) [6]. In this, the C···F hydrogen-bond interactions defined along the chains (3.08 Å) and interchains (3.27 Å) both compare well with those found in **1** for the ^{1}D and ^{2}D assemblies, of 3.06 and 3.16 Å, respectively. Therefore, as it had been proposed, the double substitution at the 3 and 5 positions on the pyrazole ring by alkyloxyphenyl substituents does not significantly modify the molecular assembly in the solid with respect to the analogous compounds containing only one substituent at the 3 position on the pyrazole ring (Fig. 1). In both cases, the tetrahedral BF_4^- anion appears to be responsible for the molecular assembly, giving rise to the formation of weak ^{2}D networks.

Complex **2** exhibits similar structural features to **1**. However, in this case, each type of interaction defining

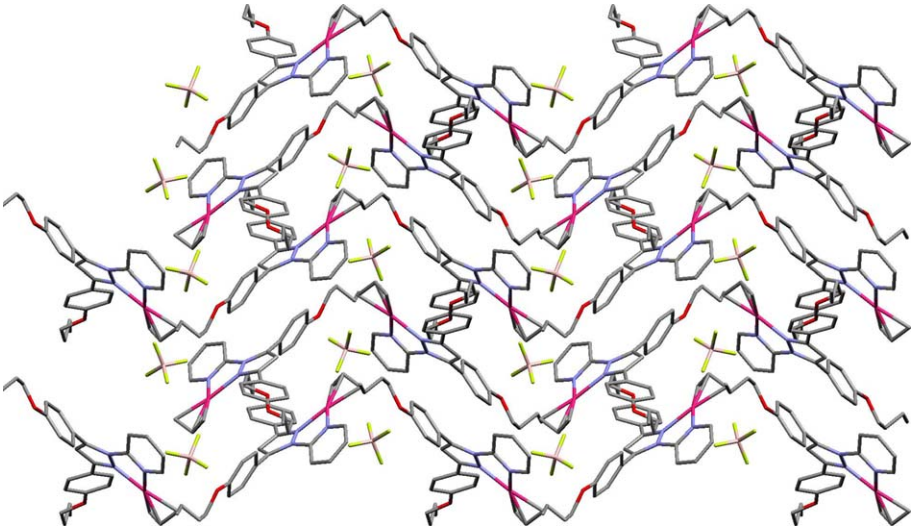

Fig. 5. View of a layer of **1** in the *ab* plane. The contacts have been omitted for clarity.

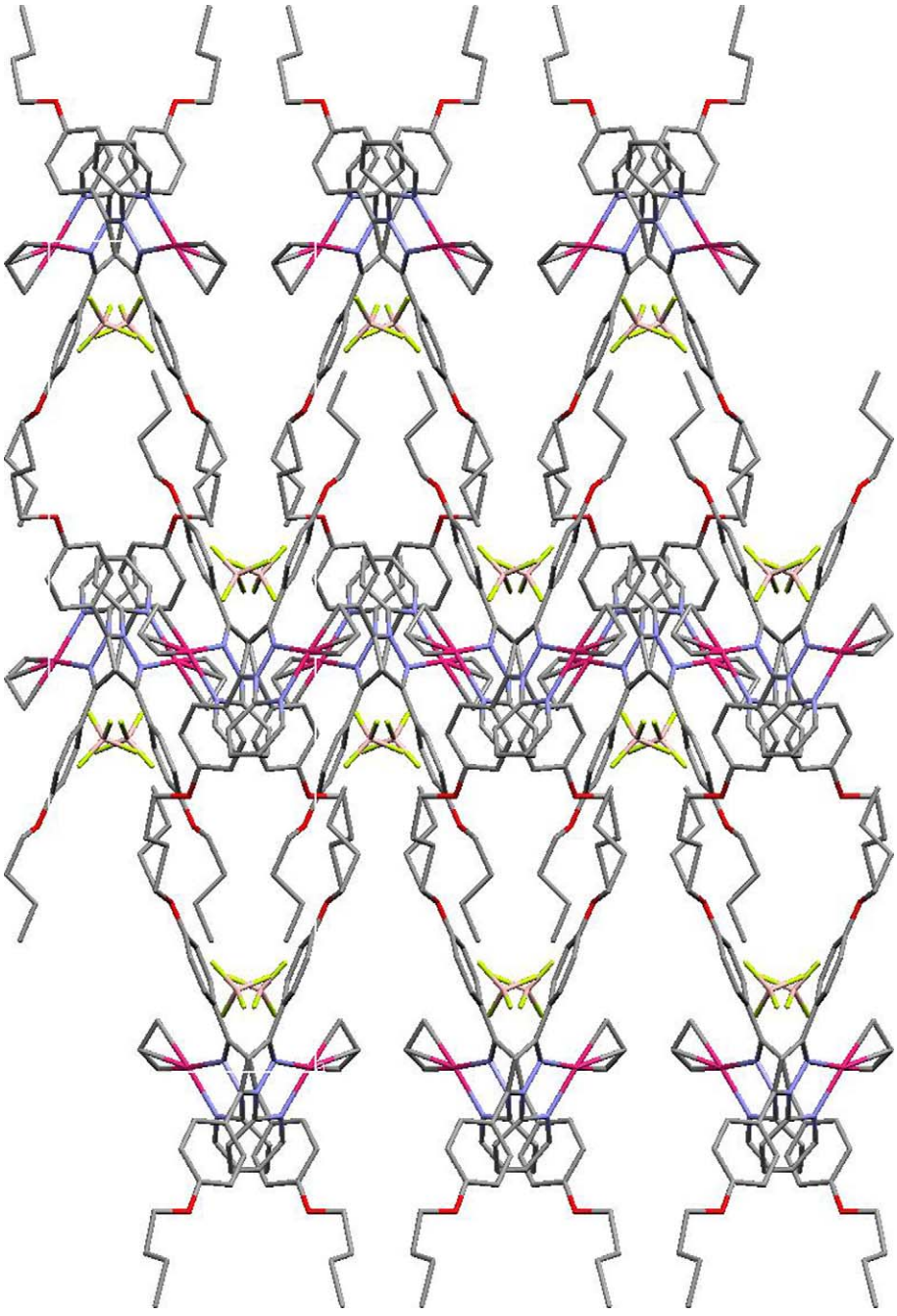

Fig. 6. ^{2}D network of **1**, showing the interdigitation of the chains between layers.

the molecular assembly presents two values because to the presence of two molecules per asymmetric unit. At the molecular level, each $[Pd(\eta^3\text{-}C_3H_5)(pz^{bp2}py)]^+$ unit in **2** interacts with its neighbouring counteranion through a weak coordinative Pd···O5 interaction of ca. 3.90 Å.

Each $[Pd(\eta^3\text{-}C_3H_5)(pz^{bp2}py)]CF_3SO_3$ entity interacts with its neighbours through weak non-conventional hydrogen-bonds, C17A···O4B$(x, y+1, z)$ of 3.22(1) Å and C17B···O3A$(x, y-1, z)$ of 3.27(1) Å (Table 3). These interactions, which are propagated along the *a* axis (Fig. 7), generate a one-dimensional arrangement with the Pd atoms showing a *zig-zag* distribution and Pd···Pd distances of ca. 6 Å.

Additional extended C···F and C···O interactions (the shortest distances are 3.27(1) and 3.33(1) Å, respectively; Table 3) give rise to layers that lie almost parallel to the *ac* plane, thus generating a ^{2}D network (Fig. 8) in which the flexible chains are interdigitated occupying the space between the layers.

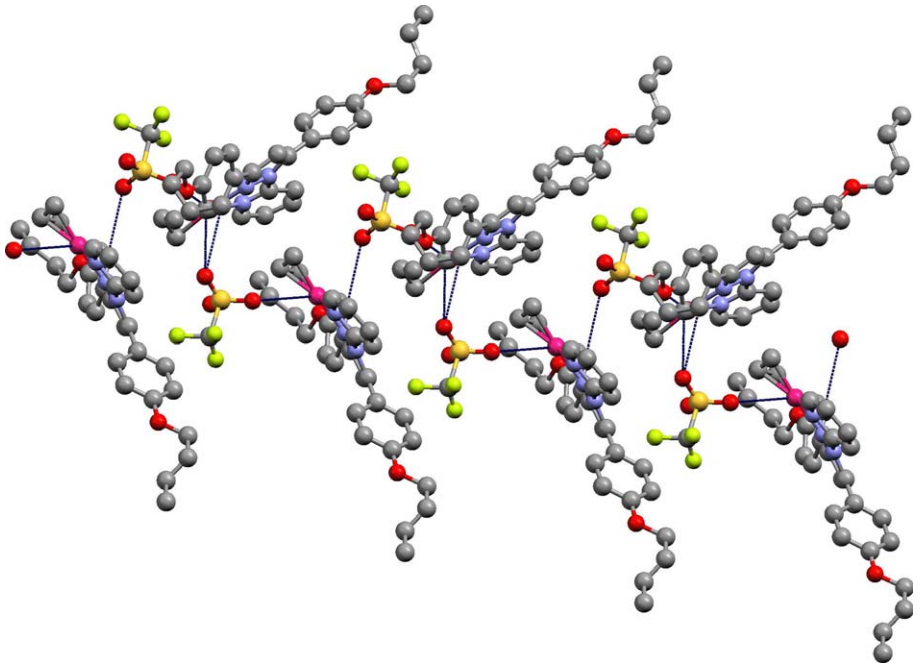

Fig. 7. View of the chain of **2** along the *a* axis, showing the Pd···O and C···O contacts.

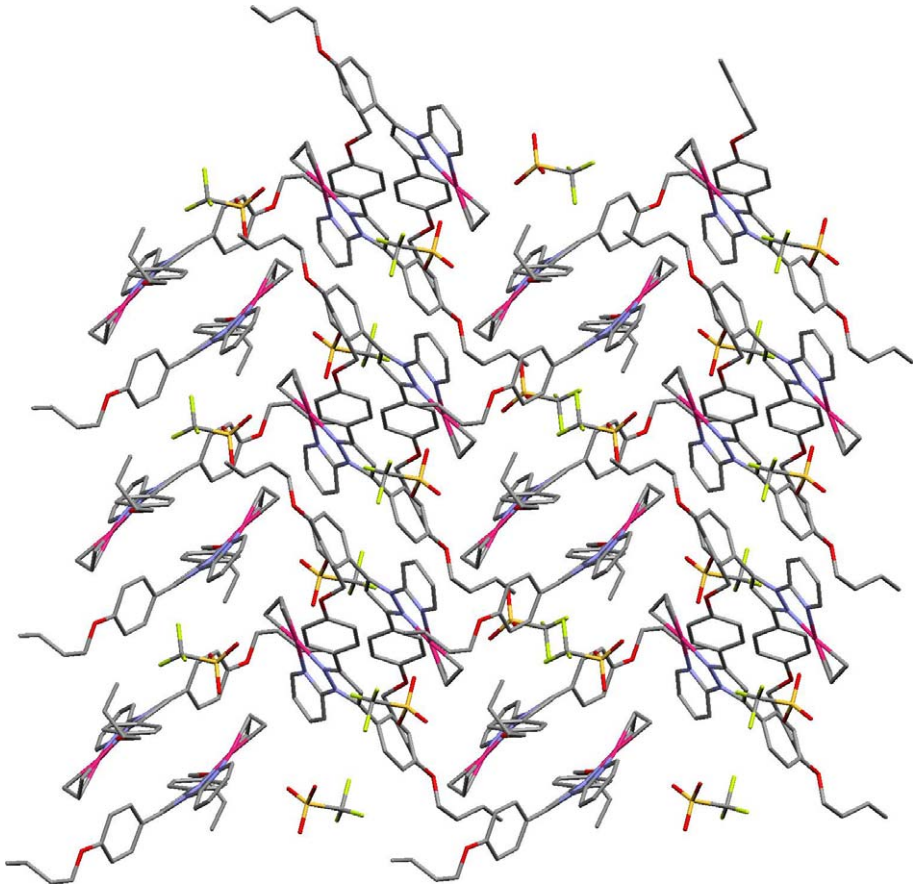

Fig. 8. ^{2}D network of **2** in the *ac* plane. The contacts have been omitted for clarity.

4. Conclusions

We have studied herein the effect of C–H···O and C–H···F hydrogen bonds on the crystal structures of $[Pd(\eta^3\text{-}C_3H_5)]^+$ complexes containing the 2-[3,5-bis(4-butoxyphenyl)pyrazol-1-yl]pyridine ($pz^{bp2}py$) ligand and BF_4^- and $CF_3SO_3^-$ as counterions (**1** and **2**, respectively). In spite of the weakness of the interactions, reflected on the C–H···O and C–H···F distances, their occurrence in the organometallic complexes studied is responsible for the generation of weak ^{2}D supramolecular networks.

The relative intermolecular orientations between the cationic metal complexes and the counterions can be traced to C–H···O and C–H···F hydrogen bonds. In particular, the orientation of the $[Pd(\eta^3\text{-}C_3H_5)(pz^{bp2}py)]^+$ along the *b* or *a* axis in **1** and **2**, respectively, can be traced to C–H···F and C–H···O/F bonding interactions related with the presence of BF_4^- or $CF_3SO_3^-$ bridging counterions, so generating *zig-zag* chains. Regarding the geometry of the counterions, the pyridine or benzene C–H donors participate in extended C–H···F and C–H···O/F interactions responsible for the interchain bonding, which give rise to layer arrangements of ^{2}D networks.

Complexes **1** and **2** are new examples which show that a detailed analysis of the nature of weak interactions should also be taken into account when designing supramolecular assemblies.

5. Supplementary data

The supplementary crystallographic data have been passed to the Cambridge Crystallographic Data Centre (CCDC deposition numbers 288062 and 288063 for **1** and **2**, respectively).

Acknowledgments

We are grateful to the Dirección General de Investigación/MEC of Spain (Project No. BQU2003-07343) for financial support. We also thank to Comunidad de Madrid for financial support (Project GR/MAT/0511/2004) and the contract to M.C.T.

References

[1] B.-H. Ye, M.-L. Tong, X.-M. Chen, Coord. Chem. Rev. 249 (2005) 545.
[2] (a) M. Eddaoudi, D.B. Moler, H. Li, B. Chen, T.M. Reineke, M. O'Keeffe, O.M. Yaghi, Acc. Chem. Res. 34 (2001) 319;
(b) B. Moulton, M.J. Zaworotko, Chem. Rev. 101 (2001) 1629;
(c) B.J. Holliday, C.A. Mirkin, Angew. Chem. Int. Ed. 40 (2001) 2023;
(d) G.F. Swiegers, T.J. Malefetse, Chem. Rev. 100 (2000) 3483;
(e) S.R. Batten, R. Robson, Angew. Chem. Int. Ed. 37 (1998) 1460;
(f) D.L. Caulder, K.N. Raymond, Acc. Chem. Res. 32 (1999) 975;
(g) K.R. Seddon, M. Zaworotko (Eds.), Crystal Engineering: The Design and Application of Functional Solids, Kluwer Academic Publishers, Dordrecht, 1996;
(h) G.R. Desiraju, Crystal Engineering: The Design of Organic Solids, Elsevier, Amsterdam, 1989.
[3] (a) C. Janiak, T.G. Scharmann, Polyhedron 22 (2003) 1123;
(b) G.R. Desiraju, Acc. Chem. Res. 35 (2002) 565;
(c) G.R. Desiraju, T. Steiner, The weak hydrogen bond in: IUCr Monograph on Crystallography, vol. 9, Oxford Science, Oxford, 1999;
(d) K.N. Houk, S. Menzer, S.P. Newton, F.M. Raymo, J.F. Stoddart, D.J. Williams, J. Am. Chem. Soc. 121 (1999) 1479;
(e) T. Steiner, Chem. Commun. (1997) 727;
(f) G.R. Desiraju, Acc. Chem. Res. 29 (1996) 441.
[4] R.M. Claramunt, P. Cornago, M. Cano, J.V. Heras, M.L. Gallego, E. Pinilla, M.R. Torres, Eur. J. Inorg. Chem. (2003) 2693.
[5] M. Cano, J.V. Heras, M.L. Gallego, J. Perles, C. Ruiz-Valero, E. Pinilla, M.R. Torres, Helv. Chim. Acta 86 (2003) 3194.
[6] M.C. Torralba, M. Cano, J.A. Campo, J.V. Heras, E. Pinilla, M.R. Torres, J. Organomet. Chem. 691 (2006) 765.
[7] M.J. Mayoral, M.C. Torralba, M. Cano, J.A. Campo, J.V. Heras, Inorg. Chem. Commun. 6 (2003) 626.
[8] J.A. Campo, M. Cano, J.V. Heras, M.C. Lagunas, J. Perles, E. Pinilla, M.R. Torres, Helv. Chim. Acta 85 (2002) 1079.
[9] Siemens, SAINT: Data Collection and Procedure Software for the SMART System, Siemens Analytical X-Ray Instrument Inc., Madison, WI, 1995.
[10] Bruker, SHELXTL, Version 6.1, Bruker Analytical X-Ray Systems, 2000.
[11] F. Gómez-de la Torre, A. de la Hoz, F.A. Jalón, B.R. Manzano, A. Otero, A.M. Rodríguez, M.C. Rodríguez-Pérez, Inorg. Chem. 37 (1998) 6606.
[12] F. Gómez-de la Torre, A. de la Hoz, F.A. Jalón, B.R. Manzano, A.M. Rodríguez, J. Elguero, M. Martínez-Ripoll, Inorg. Chem. 39 (2000) 1152.
[13] M.C. Torralba, M. Cano, S. Gómez, J.A. Campo, J.V. Heras, J. Perles, C. Ruiz-Valero, J. Organomet. Chem. 682 (2003) 26.